J Am Oil Chem Soc (2007) 84:1081–1093
DOI 10.1007/s11746-007-1141-6

ORIGINAL PAPER

Physicochemical and Rheological Properties of Crystallized Blends Containing *trans*-free and Partially Hydrogenated Soybean Oil

J. Reyes-Hernández · E. Dibildox-Alvarado · M. A. Charó-Alonso · J. F. Toro-Vazquez

Received: 1 January 2007 / Revised: 17 July 2007 / Accepted: 23 July 2007 / Published online: 15 November 2007

Abstract Three vegetable oil blends, intended for formulation of high melting temperature confectionary coatings, were prepared by mixing different proportions of coconut oil, palm stearin, and either partially hydrogenated soybean oil (PH-SBO) or native soybean oil (i.e., *trans*-free SBO). The blends were crystallized under the same isothermal conditions and the crystallized systems evaluated by DSC, SFC, polarized light microscopy, and rheology under low [i.e., G′ and yield stress (σ^*)] and high (i.e., creep and recovery profiles) stress forces. Overall, all *trans*-free blends showed lower SFC and heat of crystallization than the ones obtained with PH-SBO blends. These results showed that *trans*-fatty acids decrease the level of structural order of the crystals, and probably also the organization of the crystal network. As a result, most of the crystallized blends with PH-SBO showed lower σ^* values and higher creep profiles (i.e., softer texture) than *trans*-free blends, particularly in systems crystallized at high supercooling and blends with saturated medium chain TAG. Nevertheless, at particular crystallization temperatures some *trans*-free formulations provided crystallized systems with rheological properties that would result in softer textures than the ones obtained with PH-SBO blends. Knowledge of the rheological properties under low and high stress forces is vital when comparing the functionality of crystallized TAG systems with and without TAG with *trans*-fatty acids.

Keywords Fat crystallization · Lipid chemistry/lipid analysis · Rheology · Thermal analysis

J. Reyes-Hernández · E. Dibildox-Alvarado · M. A. Charó-Alonso · J. F. Toro-Vazquez
Facultad de Ciencias Químicas-CIEP,
Universidad Autónoma de San Luis Potosí,
San Luis Potosí, Mexico

J. Reyes-Hernández
Facultad de Química,
Universidad Autónoma de Querétaro,
DIPA-PROPAC, Querétaro, Mexico

J. F. Toro-Vazquez (✉)
Facultad de Ciencias Químicas,
Zona Universitaria,
Av. Dr. Manuel Nava 6,
San Luis Potosí 78210, Mexico
e-mail: toro@uaslp.mx

Vegetable oils are the most important edible lipids worldwide. However, most vegetable oils lack the required functional properties to meet consumer demands for texture and stability in food products. Thus, at the beginning of the twentieth century hydrogenation of vegetable oils was developed to improve their plasticity and oxidation stability properties [1]. Today, partial hydrogenated vegetable oils are used worldwide in the formulation of functional shortenings and confectionary coatings. Unfortunately, partial hydrogenation of vegetable oils results in the production of *trans* fatty acids that once ingested have detrimental effects on metabolic functions, resulting in altered cell membrane integrity and reduced production of biologically active metabolites derived from essential fatty acids [2, 3]. *Trans* fatty acids in the diet have additional health implications because their impact on the ratio of high density to low density lipoproteins [4], and their high consumption is a rate-limiting factor for the Δ6-desaturase that converts the α-linoleic fatty acid into γ-linoleic in the metabolic pathway of the ω-6 series [5]. As a result, public

health agencies such as the World Health Organization, the American Heart Association, and the Dietary Guidelines 2005, issued recommendations to limit *trans* fat intake [6]. In the same way, the FDA set January 1, 2006 as the date by which all marketed foods must include *trans* fat concentration in the Nutrition Facts panel. All these facts are influencing manufacturers to eliminate or reduce *trans* fats from their products [6]. However, replacing partially hydrogenated vegetable oils in food products, particularly in shortening and confectionary coatings, is a difficult task since the appropriate SFC, plasticity, liquid oil entrapment, and rheological properties are hard to achieve without the presence of *trans* fatty acids.

The industry uses different approaches to reduce or eliminate the use of *trans* fats in the formulations. Some of them include the use of vegetable oils with modified TAG composition through conventional plant breeding or genetic engineering, tailored to provide specific functional properties to food systems. Other alternatives include the use of oils after interesterification with high melting temperature TAG fractions to modify the native TAG fatty acid composition and distribution, improving SFC and plasticity [7, 8]. The use of fractions of TAG with particular crystallization and melting profiles, obtained from vegetable oils by fractional crystallization, is another common alternative to avoid the use of *trans* fats [9, 10]. Additionally, new hydrogenation methods are now being used or investigated to reduce *trans* fatty acids' production [11, 12] or to promote the production of conjugated fatty acids with recognized health benefits [13]. Unfortunately, these approaches do not easily provide the oils and/or fats with the physical and chemical properties required to manufacture all food products where TAG are main functional components. In other cases, the use of these alternatives results in higher costs.

The most important characteristics that favors the use of partially hydrogenated fats and oils by the industry, is a higher crystallization temperature followed by a rapid crystallization rate in comparison with the ones observed by *trans*-free alternatives. Additionally, the crystallization process of *trans* TAG results in the development of a 3-dimensional crystal network that provides the appropriate functional properties (i.e., texture) and oxidation stability to the system. In the particular cases of confectionery fats and shortenings, replacing *trans* fats with *trans*-free formulations always has the shortcoming of limited plasticity, texture profile, and stability that are usually resolved with the use of palm oils, palm kernel oils or their stearin fractions [14]. All these vegetable oils have high concentration of saturated fatty acids, such as palmitic and lauric acid, with recognized cholesterolemic effect on humans. Nevertheless, the comparative analysis made by Ascherio et al. [15] of nine independent human clinical trials, supports the use of fats with saturated fatty acids over the ones containing *trans* fatty acids. After comparing the change in the ratio of low density lipoproteins to high density lipoproteins as a function of the percentage of energy provided by *trans* or saturated fatty acids, Ascherio et al. [15] concluded that *trans* fatty acids have an adverse effect on coronary heart disease risk higher than saturated fatty acids.

The objective of this investigation was to compare the crystallization and rheological properties of vegetable oil blends with *trans*-fatty acids with those of *trans*-free blends. The blends with *trans*-fatty acids were prepared with coconut oil, palm stearin, and partially hydrogenated soybean oil (PH-SBO), and the *trans*-free blends were prepared by replacing the PH-SBO with native soybean oil (*trans* free SBO). A particular requirement of the blends developed was a high melting temperature profile (45–52 °C), since the final aim of use is in the formulation of *trans*-free high melting temperature confectionary coatings.

Materials and Methods

Vegetable Oils Analysis

The natural soybean oil (i.e., *trans*-free SBO), PH-SBO, coconut oil, and palm stearin were obtained from local distributors. All oils were heated (80 °C for 20 min), vacuum filtered (Whatman paper No. 5) and then stored (4 °C) under nitrogen in the dark. Oil samples were analyzed for fatty acids and TAG profiles by capillary-GC and HPLC, respectively. Capillary-GC was done in a Shimadzu GC-2010 (Shimadzu Corp., Kyoto, Japan) coupled with a gas flow controller (Shimadzu TCD-2010) and a flame ionization detector. The column was a 100 m fused silica WCOT (VARIAN CP7420) with an internal diameter of 0.25 mm at a temperature of 180 and 250 °C in the injector and the detector. The volume injected was 1 μL with a 1:100 split, using Helium as the carrier gas (1 mL/min). HPLC analyses were performed as reported by Pérez-Martínez et al. [16].

Blend Formulation

The blends investigated were selected from an initial exploratory study (unpublished) consisting in blending different proportions (0–100% wt/wt) of PH-SBO, coconut oil, and palm stearin (Table 1). The proportions of the oils in the blends were obtained through a three-component axial experiment design [17]. Blends with a melting temperature by DSC between 45 °C and 52 °C were selected

Table 1 Vegetable oil proportions in the selected blends

	Soybean oil (%)[a]	Coconut oil (%)	Palm stearin (%)
Blend 5	50.0	0.0	50.0
Blend 7	33.3	33.3	33.3
Blend 10	16.7	16.7	66.6

[a] Blends were developed with *trans*-free soybean oil or with partially hydrogenated soybean oil (PH-SBO)

for this investigation. The selected blends corresponded to the ones coded as blend 5, blend 7, and blend 10 (Table 1). Blends with similar proportions among the three oil components were prepared, replacing the PH-SBO with *trans*-free SBO.

Calorimetry and SFC Analysis

Dynamic calorimetric analyses were done in a DSC TA Instruments Model 2920 (TA Instruments, New Castle, Delaware, USA) coupled with a TA Instruments RCS cooling system. The equipment was calibrated as previously indicated [18]. Samples (0.8 mg) of the blends were sealed in aluminum pans held at 80 °C for 20 min and then cooled down (1.0 °C/min) from 80 to −30 °C. After 1 min at −30 °C the melting thermogram was obtained at a rate of 5.0 °C/min. The temperatures at the beginning of crystallization and the end of melting (T_e) were calculated with the equipment software (TA-Instruments Universal Analysis 2000, v. 4.0) using the first derivative of the heat flux. For each blend two independent determinations were done.

The selected blends (blend 5, 7 and 10 with either PH-SBO or *trans*-free SBO) were analyzed by DSC under isothermal conditions. The blends were first held for 20 min at 80 °C and then cooled (1 °C/min) at the corresponding crystallization temperature (T_{Cr}). After completion of the crystallization exotherm (i.e., heat capacity returned to the baseline) the system was left for additional 30 min and then the melting thermogram was determined (5 °C/min). Two independent determinations were done at each T_{Cr}. The T_{Cr}'*s* used in the isothermal crystallization studies were in the interval between the temperatures at the beginning of crystallization, from the corresponding dynamic crystallization thermogram, up to 6 °C above this temperature. The use of isothermal T_{Cr}'*s* above this temperature interval produced a significant increase in the induction time of crystallization and broadened the exotherm, making difficult to establish the beginning and end of crystallization. From the isothermal crystallization thermograms we calculated the induction time of crystallization (t_i) as the time where the first derivative of the heat capacity of the sample initially departed from the base line, and the heat of crystallization (ΔH_{Cr}) as the area under the exotherm. On the other hand, the melting thermogram was characterized calculating the temperature at the peak of the endotherms (T_{pk}), the corresponding heat of fusion (ΔH_{pk}), and the temperature at the end of melting (T_M). As with the crystallization thermogram, all these parameters were determined with the equipment software using the first derivative of the heat flux. Finally, following the AOCS direct method [19], the SFC of both types of blends, i.e., with PH-SBO and with *trans*-free SBO, was determined at 5 °C intervals between 15 and 55 °C (SFC_{AOCS}). For all measurements two independent determinations were done.

Rheometry Analysis

The elasticity (G′) and the yield stress (σ^*) of the crystallized blends were determined with a mechanical spectrometer equipped with a 50-mm diameter parallel plates geometry (Paar Physica UDS 200, Stuttgart, Germany). Temperature was controlled by a Peltier system located on the base of the measurement geometry. The melted blend (80 °C) was applied on the base of the plate avoiding bubble formation and the superior plate was positioned on the sample surface using the auto-gap function of the rheometer software (1 mm). After erasing the crystallization memory (80 °C for 20 min) the system was cooled at 1 °C/min to corresponding T_{Cr} then crystallized over 200 min. A constant deformation (0.1%) with a constant angular frequency (1 rad/s) was and the G′ and G″ measured. The total time of crystallization was considered the equilibrium time of crystallization and the rheological parameters the equilibrium values (i.e., G_{eq}' and G_{eq}''). In the same way, after 200 min of isothermal crystallization of the blends an oscillatory stress ramp (increasing logarithmically from 0.001 to100% deformation in 2 min) was applied with an angular frequency of 1 rad/s. The σ^* was determined from the log–log plot of shear stress vs. strain (%) at the corresponding upper limit of strain within the linear viscoelastic region. The G_{eq}', G_{eq}'', and σ^* parameters characterized the rheological properties of the crystallized blends at rest.

In an independent analysis, the viscoelasticity of the crystallized blend was evaluated through determination of the creep and recovery profile as follows. After 200 min of isothermal crystallization at T_{Cr}, a force of 10 Pa was applied for 1 min to the crystallized blend measuring the deformation (% strain). After this time, the force was withdrawn while the deformation measurements continued for an additional 25 min. The creep (i.e., slow and progressive deformation of the material under constant stress) and the recovery (i.e., value of the strain following release of the stress) profile at each T_{Cr} was evaluated by plotting

the corresponding deformation (% strain) of the crystallized blend as a function of time under constant stress. The force applied (i.e., 10 Pa) was selected based in the σ^* profiles obtained for the crystallized blends and exploratory creep and recovery measurements. A too high a force produced a fast and high deformation with very small recovery. On the other hand, a too small a force resulted in limited deformation of the material, resulting in practically the same creep and recovery profiles even between different crystallized blends.

Microstructure

Polarized light microphotographs (PLM) of the crystallized blends were obtained using a polarized light microscope (Olympus BX51; Olympus Optical Co., Ltd., Tokyo, Japan) equipped with a color video camera (KP-D50; Hitachi Digital, Tokyo, Japan) and a single ramp temperature controller (TP94; Linkam Scientific Instruments, Ltd., Surrey England) connected to a heating/freezing stage (LTS 350; Linkam Scientific Instruments, Ltd.) and a liquid nitrogen tank. Additional details for the technique are described elsewhere [16].

Experimental Design and Statistical Analysis

The treatments investigated in blends 5, 7, and 10 resulted from the factorial combination of two types of soybean oil (i.e., *trans*-free SBO or PH-SBO) and four levels of T_{Cr}. The treatments were distributed in a complete aleatory experiment design with two replicates and the results analyzed by ANOVA and contrast among the treatment means using STATISTICA V 7.1 (StatSoft Inc., Tulsa, OK, USA). The response variables investigated included t_i, ΔH_{Cr}, T_{pk1}, ΔH_{pk1}, T_{pk2}, ΔH_{pk2}, and T_M.

Results

TAG Composition and Dynamic DSC

Table 3 shows the fatty acids profile (including *cis* and *trans* fatty acid isomers) for PH-SBO and *trans*-free SBO. However, given the wide variety of *trans* fatty acids isomers present in PH-SBO it was not possible to establish a reliable TAG profile for this vegetable oil. From the fatty acid composition it was evident that the partial hydrogenation applied to the soybean oil, resulted in the production of *trans*-fatty acids, *cis/trans* isomers of 18:2 and 18:3, and oleic acid, along with a small proportion of stearic acid (Table 3).

As expected, the onset of crystallization and end of melting of the vegetable oils used in the blends formulations (Fig. 1) was directly associated with the concentration of saturated and unsaturated fatty acids of the major TAG present in the vegetable oils (Table 2). Coconut oil showed a sharp and narrow crystallization exotherm with a crystallization onset 12 °C (Fig. 1a) associated with its high content of TAG with medium chain fatty acids (Table 2). The corresponding melting thermogram had two overlapped endotherms with peak temperatures at ≈6 °C and ≈23 °C, and T_e of ≈27 °C (Fig. 1b). The DSC results for palm stearin agreed with the DSC and X-ray diffraction studies of Sonoda et al. [20]. Thus, the exothermic peaks around 31 °C and 3 °C were associated with α crystallization of high and low melting TAG fractions, the exotherm around 21–22 °C was associated to the development of a β' polymorph (Fig. 1a), while the endotherms were associated to melting of α (≈3 °C), melt mediated transformation from α to β' (15–25 °C), and melting of β' (≈36 °C) and β' (≈53 °C) polymorphs [20] (Fig. 1b). PH-SBO and *trans*-free SBO showed different crystallization (Fig. 1a) and melting (Fig. 1b) thermograms. PH-SBO had higher content of saturated fatty acids and lower concentration of linoleic and linolenic fatty acids than *trans*-free SBO (Table 3). Additionally, *trans* fatty acids present in PH-SBO and absent in *trans*-free SBO have, in general, higher crystallization and melting temperature than *cis* fatty acids present in native SBO (Table 3). Therefore, the onset of crystallization for PH-SBO was around 0 °C, while for *trans*-free SBO was ≈−9 °C with T_e's of ≈17 °C and −5 °C, respectively (Fig. 1).

It is important to establish that the blends were a mixture of TAG families with different properties (i.e., unsaturation extent, isomerism, solubility in the liquid phase, melting temperature). Their crystallization behavior was determined through interactions among physical and chemical variables, some of these directly associated to the characteristics of the blends' formulation (i.e., concentration of TAG families, melting temperature and structural compatibility between TAG families) while others were processing variables such as T_{Cr}, supercooling, and cooling rate. Within this context, blends with PH-SBO had higher SFC_{AOCS} than the ones with *trans*-free SBO (Fig. 2). This was particularly evident at temperatures lower than 40 °C ($P < 0.05$) for the blends with the higher proportion of palm stearin (i.e., blend 5 and 10), and at temperatures lower than 25 °C for the blend with the lowest proportion of palm stearin and highest proportion of coconut oil (i.e., blend 7) (see Table 1; Fig. 2). Independent of the presence of PH-SBO and crystallization temperature, the SFC_{AOCS} followed a direct relationship with the concentration of high melting temperature TAG in the blends (e.g., PPP) (Table 1). Then, blend 10 had the highest SFC_{AOCS},

Table 2 Triacylglyceride (TAG) concentration profiles for palm stearin, coconut oil and *trans*-free soybean oil (*trans*-free SBO)

TAG[a]	Palm stearin[b]	Coconut oil	*trans*-free SBO
CaCaCa/CyLaLa		2.00 (0.01)	
CyLaLa/CaCaLa/CyLaM		12.87 (0.25)	
CaCaM/CaLaLa		19.66 (0.32)	
LaLaLa		23.76 (0.07)	
CaLaM		0.65 (0.04)	
LaLaM	0.05 (0.00)	18.88 (0.08)	
MPO/MPLn	0.50 (0.06)		
MMM/LnLnLn	0.06 (0.01)		
LaLaO		1.54 (0.03)	
LaMM		10.38 (0.04)	
LaMO		1.28 (0.01)	
LaMP/MMM		4.43 (0.21)	
LaMP/LaPP/MPO		1.28 (0.02)	
LnLeLn			4.77 (0.34)
LnLnLn			19.92 (0.16)
LnLeO			3.74 (0.12)
LnLeP			1.63 (0.07)
LnLnO			20.22 (0.13)
LnLnP			15.49 (0.15)
OLnO			8.98 (0.10)
LnLnSt			3.27 (0.15)
OLnP			10.16 (0.11)
OOLn	0.26 (0.31)		
PLnO	5.32 (0.25)		
PPLn	5.68 (0.28)		
PLnP			1.41 (0.06)
OOO	0.79 (0.08)		3.13 (0.17)
OLnSt			2.38 (0.04)
OOP			2.09 (0.04)
POO	18.71 (0.16)		
PLnSt			0.96 (0.05)
POP			0.36 (0.03)
PPO/POP	39.12 (0.62)		
PPP	20.47 (0.64)		
OOSt	3.10 (0.16)		0.57 (0.02)
POSt	1.96 (0.64)		0.37 (0.10)
StLSt	0.13 (0.05)		0.14 (0.10)
StOSt	0.09 (0.06)		
Unidentified	3.79 (0.23)	3.29 (0.02)	0.41 (0.02)

[a] *Cy* caprylic, *Ca* capric, *La* lauric, *M* myristic, *P* palmitic, *Po* palmitoleic, *St* stearic, *O* oleic, *Ln* linoleic, *Le* linolenic, *A* arachidic

[b] All results are reported as a percentage of the total area. Mean and standard deviation of at least two replicates ($n = 2$)

followed by blend 5 and then blend 7 ($P < 0.05$). Regarding the melting profiles, all blends had T_e'*s* between 48 °C and 54 °C (Fig. 3) with blend 10 showing the highest T_e (≈54 °C), followed by blend 5 (≈51 °C), and then blend 7 (≈48 °C). However, at temperatures lower than 40 °C blends with PH-SBO showed larger endotherms than blends with *trans*-free SBO (Fig. 3). This behavior was associated with the higher SFC_{AOCS} present in blends with PH-SBO than in *trans*-free blends. PH-SBO and its blends had higher concentration of saturated TAG and TAG with unsaturated *trans* fatty acids, i.e., elaidic, vaccenic, or *cis-trans* isomers of 18:2 (Table 3) both with higher melting temperature than *cis* fatty acids.

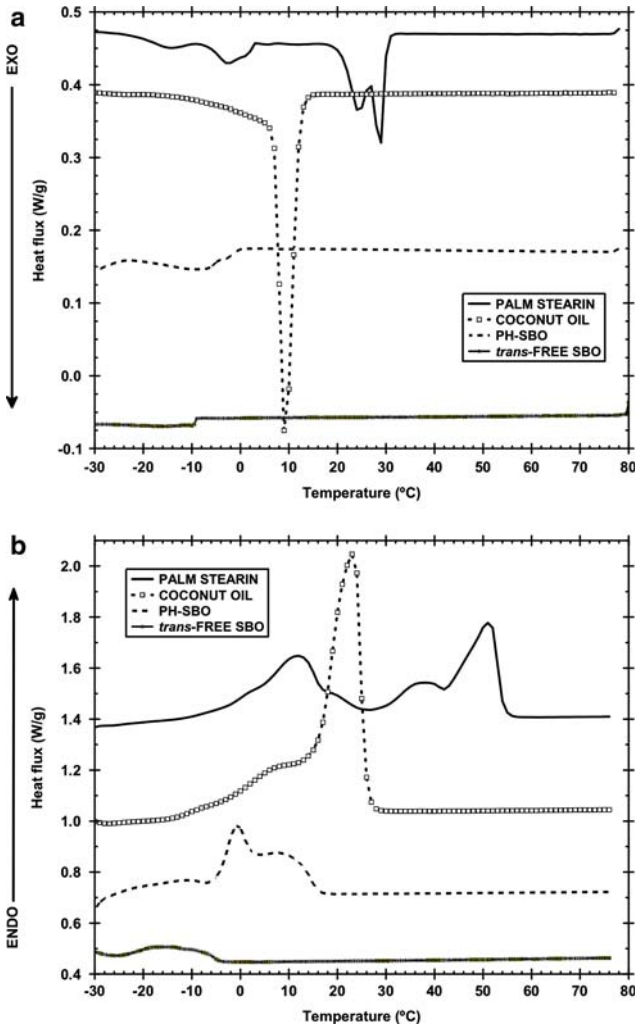

Fig. 1 Dynamic crystallization (**a**) and corresponding melting thermograms (**b**) for the vegetable oils used in this investigation

Isothermal Crystallization of the Selected Blends

The cooling rate used to attain isothermal conditions was low and possibly the crystallization process (i.e., nucleation) started even before achieving T_{Cr}. However, DSC did not detect this process in any of the blends

Table 3 Fatty acids concentration profile for partially hydrogenated soybean oil (PH-SBO) and *trans*-free soybean oil (*trans*-free SBO)

Fatty acid[a]	Formula (positions of *cis/trans* double bonds)	PH-SBO[b]	*trans*-free SBO[b]
Lauric	12:0	0.12 (0.00)	–
Myristic	14:0	0.21 (0.00)	0.10 (0.02)
Palmitic	16:0	14.10 (0.22)	11.39 (1.78)
Palmitoleic	16:1 (9*c*)	0.09 (0.00)	0.09 (0.02)
Stearic	18:0	4.43 (0.11)	3.98 (0.16)
trans Isomers of 18:1	18:1 (8,10,11,12,13)	15.74 (0.00)	–
Oleic	18:1 (9*c*)	32.67 (0.61)	22.73 (0.43)
cis isomers of 18:1	18:1 (10,11,12,13,14,15)	7.83 (0.81)	1.33 (0.01)
Linoleic	18:2 (9*c*, 12*c*)	18.13 (0.33)	53.47 (0.96)
cis/trans isomers of 18:2	18:2 (*tt, ct, tc*)	3.59 (0.03)	–
Linolenic	18:3 (9*c*, 12*c*, 15*c*)	1.45 (0.13)	6.56 (0.21)
cis/trans isomers of 18:3	18:3 (*ttt, tct, ctc, ctt, tct, cct, ttc, ctc, tcc*)	2.53 (0.15)	–
Arachidic	20:0	0.43 (0.13)	0.27 (0.06)
Unidentified	–	0.13 (0.00)	0.08 (0.00)
Total percent			
Saturated fatty acids		19.38 (0.46)	15.83 (2.03)
Unsaturated fatty acids		58.76 (1.75)	84.17 (1.78)
trans fatty acids		15.74 (0.00)	–
cis/trans isomers of 18:2 and 18:3		6.12 (0.33)	–

[a] *Cy* caprylic, *Ca* capric, *La* lauric, *M* myristic, *P* palmitic, *Po* palmitoleic, *St* stearic, *O* oleic, *Ln* linoleic, *Le* linolenic, *A* arachidic

[b] All results as a percentage of the total area. Mean and standard deviation of at least two replicates ($n = 2$)

investigated. When blends were isothermally crystallized, just one exotherm was obtained (data not shown), showing the classical crystallization behavior, i.e., the lower the T_{Cr} the shorter the t_i and the larger the ΔH_{Cr} (Tables 4 and 5). The only exception was blend 5 with both PH-SBO or *trans*-free SBO, where decreasing T_{Cr} from 28 to 26 °C produced both a reduction in t_i and ΔH_{Cr}. This suggested that at T_{Cr} = 28 °C blend 5 with or without TAG with *trans* fatty acids developed a different polymorph than at 26 °C. Unfortunately, no X-ray analysis was done to corroborate this.

In general, for a given blend t_i had a tendency to be smaller in *trans*-free SBO blends than in PH-SBO blends (Tables 4 and 5). It is well known that t_i is inversely associated to the rate of nucleation and has an inverse relationship with supercooling (i.e., $T_{Cr} - T_M$). However, such t_i differences could not be associated with the supercooling effect since for the same blend and for most T_{Cr}'*s* investigated, T_M was the same for the blends with or without *trans* fatty acids (Tables 4 and 5). In the blends t_i may be affected by the structural compatibility between TAG with *cis* or *trans* unsaturations and the saturated TAG. Thus, in *trans*-free blends the saturated TAG families with the higher melting temperature (i.e., LaLaLa from coconut oil and PPP from palm stearin; Table 2) might be segregated from the liquid phase formed mainly by TAG with high degree of *cis* unsaturations (i.e., LnLnLn, LnLnO from soybean oil; Table 2). This, due to the structural incompatibility between TAG with *cis* unsaturations and the saturated TAG. In contrast, *trans* fatty acids are structurally more similar to saturated fatty acids than *cis* fatty acids and in PH-SBO blends the saturated TAG lamellae might incorporate unsaturated *trans* TAG, resulting in lamellae with mixed composition but slower nucleation rates (i.e., longer t_i) than in *trans*-free blends. Within this framework, t_i was smaller in *trans*-free blends than in PH-SBO blends (Tables 4 and 5). However, such difference was not statistically significant for blend 5 at any of the T_{Cr} investigated, and for blends 7 and 10 was significant just at the higher T_{Cr} ($P < 0.05$) (Tables 4 and 5).

All PH-SBO blends observed at all T_{Cr}'*s* investigated significant smaller ΔH_{Cr} values ($P < 0.05$) than the corresponding ΔH_{Cr} for *trans*-free blends (Tables 4 and 5). This indicated that crystals in the *trans*-free blends achieved a higher level of structural order than PH-SBO blends. As previously mentioned, unsaturated TAG with *trans* fatty acids are more structurally compatible with saturated TAG than the *cis*-unsaturated TAG. Then, mixed crystals formed by saturated TAG and unsaturated *trans* TAG would have a lower level of order (i.e., lower ΔH_{Cr}) than the crystals developed just by saturated TAG. The difference between the ΔH_{Cr} values of *trans*-free blends (Table 4) and PH-SBO blends (Table 5) was even larger for blends containing coconut oil (i.e., blends 10 and 7; Table 1). The incorporation of saturated medium chain TAG (i.e., LaLaLa) into the crystals seemed to further decrease the level of structural organization and hence the heat released on crystallization.

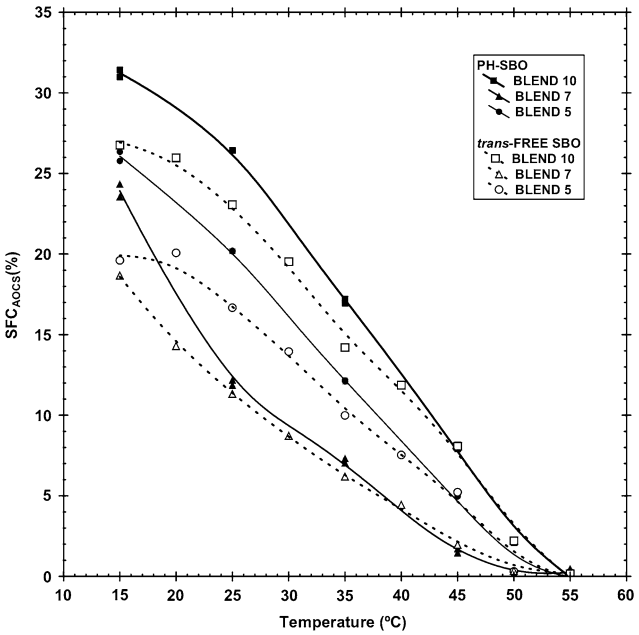

Fig. 2 Solid fat content by the official method (SFC_{AOCS}) of the selected blends with partially hydrogenated soybean oil (PH-SBO) and *trans*-free soybean oil (*trans*-free SBO). Blends formulation as indicated in Table 1

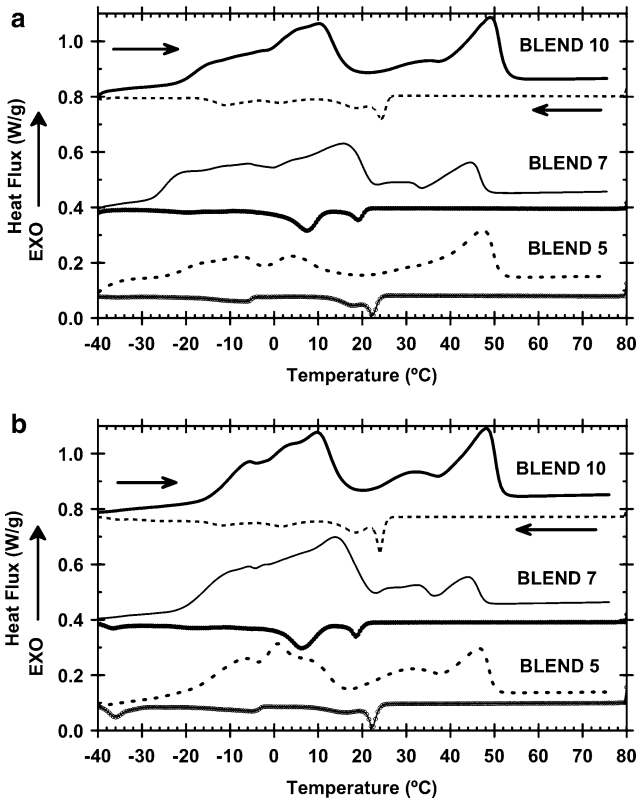

Fig. 3 Dynamic crystallization (left arrow) and melting thermograms (right arrow) of the selected blends with *trans*-free SBO (**a**) and PH-SBO (**b**). Blends formulation as indicated in Table 1

After isothermal crystallization the melting thermograms of blends 5 and 7 with both PH-SBO and *trans*-free SBO showed two well-defined endotherms, particularly in the blends crystallized at the lower T_{Cr}'s (data not shown). In contrast, blend 10 with *trans*-free SBO or PH-SBO showed just one endotherm (data not shown). Overall and independent of the blend formulation, incorporation of *trans* TAG into the crystals developed by PH-SBO blends decreased their heat of fusion (i.e., ΔH_{pk1}, ΔH_{pk2}) when compared with the one of crystals developed by saturated TAG in *trans*-free blends (Tables 4 and 5). These results agreed with the behavior of ΔH_{Cr} discussed above. Nevertheless, the effect of *trans* TAG on crystal organization was not evident as changes in melting temperature (T_{pk1}, T_{pk2}, or T_M; Tables 4 and 5). These results contrast with the findings of Hagemann and Tallent [21] and Kodali et al. [22] that showed that β crystals of saturated TAG have higher heat of fusion and melting temperature than their corresponding *trans*-unsaturated TAG. However, these authors worked in systems with pure mono-acid TAG, while the blends here investigated were mixtures of TAG families.

Low Deformation Rheology

The G_{eq}' and σ^* profiles as a function of SFC_{eq} for the blends selected are shown in Fig. 4 in a log-log format. For all blends $Log(G_{eq}')$ and $Log(\sigma^*)$ increased with $Log(SFC_{eq})$ regardless of the type of SBO used. The statistical analysis of SFC_{eq} values showed that the higher the concentration of PH-SBO in the blends' formulation the larger the difference in SFC_{eq} between the system with and without *trans*-free SBO ($P < 0.05$). Additionally, for a particular blend this phenomenon was more evident as T_{Cr} decreased, since more *trans*-TAG, present just in the PH-SBO, solidified in the system. Then, for a particular blend and T_{Cr} the higher SFC_{eq} present in the system with PH-SBO resulted in higher G_{eq}' than in the system with *trans*-free SBO, particularly as T_{Cr} decreased (and SFC_{eq} increased). This was more evident for blend 5 (Fig. 4a), the blend with the highest concentration of PH-SBO in the formulation (i.e., 50% of PH-SBO). This again showed that high melting temperature TAG present in palm stearin (e.g., PPP), had a significant effect on blends' crystallization and subsequently in their rheological profile. Importantly, Fig. 4 showed that similar rheological properties were obtained for blends 10 and 5 (prepared with both types of SBO), even though blend 5 had lower SFC_{eq} (Fig. 4). We might therefore obtain crystallized blends with similar rheological behavior with or without the use of TAG with *trans* fatty acids. In the particular case of blend 5 the relationship between the rheological parameters and SFC_{eq} seemed to be affected by polymorphism. As

Table 4 Parameters that describe the isothermal crystallization and corresponding melting profile of the selected blends with *trans*-free SBO. Melting after isothermal crystallization at the indicated crystallization temperature (T_{Cr}). Legends as indicated in the text

T_{Cr} (°C)	t_i* (min)	ΔH_{Cr} (J/g)	T_{pk1} (°C)	ΔH_{pk1} (J/g)	T_{pk2} (°C)	ΔH_{pk2} (J/g)	T_M (°C)
Blend 5							
26	$1.00^{a,a}$ (0.11)	$19.38^{a,a}$ (3.62)	$40.38^{a,a}$ (0.04)	$12.56^{a,a}$ (1.06)	$49.48^{-,a}$ (0.00)	$4.18^{-,a}$ (1.22)	$54.19^{a,a}$ (0.71)
28	$1.65^{a,a}$ (0.24)	$24.50^{b,b}$ (1.50)	$43.93^{b,b}$ (0.06)	$25.40^{b,b}$ (0.25)			$52.46^{b,b}$ (0.07)
30	$3.57^{b,b}$ (0.45)	$21.81^{a,a}$ (2.40)	$44.96^{c,c}$ (0.22)	$22.75^{b,b}$ (3.54)			$52.77^{b,b}$ (1.07)
32	$6.97^{c,c}$ (1.59)	$17.79^{c,c}$ (2.44)	$47.34^{d,e}$ (0.18)	$22.23^{b,b}$ (1.27)			$55.42^{c,c}$ (0.11)
Blend 7							
23	$1.91^{a,a}$ (0.11)	$17.71^{a,a}$ (0.028)	$34.58^{a,a}$ (0.34)	$7.92^{a,a}$ (1.49)	$46.62^{a,a}$ (0.11)	$3.96^{a,a}$ (0.19)	$51.91^{a,a}$ (0.58)
24	$2.14^{a,a}$ (0.43)	$17.42^{a,a}$ (0.53)	$39.98^{b,b}$ (0.06)	$14.48^{b,b}$ (0.35)	$47.56^{b,b}$ (0.04)	$0.60^{b,b}$ (0.08)	$52.19^{b,b}$ (0.32)
26	$3.78^{b,b}$ (0.17)	$15.50^{b,b}$ (0.35)	$41.97^{c,c}$ (0.06)	$15.01^{b,b}$ (0.26)	$50.09^{c,-}$ (1.17)	0.02^{c} (0.005)	$51.64^{a,a}$ (0.20)
28	$7.21^{c,c}$ (1.16)	$14.93^{b,b}$ (0.82)	$43.38^{d,d}$ (0.18)	$15.24^{b,b}$ (0.07)	$51.76^{d,-}$ (1.57)	0.02^{c} (0.003)	$53.37^{b,b}$ (0.58)
Blend 10							
30	$2.67^{a,a}$ (0.33)	$33.51^{a,a}$ (0.40)	$45.17^{a,a}$ (0.08)	$27.32^{a,a}$ (0.90)			$53.74^{a,a}$ (0.67)
31	$3.28^{a,a}$ (0.33)	$31.15^{b,b}$ (0.38)	$45.56^{b,b}$ (0.01)	$28.33^{a,a}$ (1.13)			$55.37^{b,b}$ (0.46)
32	$3.96^{a,a}$ (0.25)	$30.63^{b,b}$ (0.35)	$46.05^{c,c}$ (0.12)	$27.79^{a,a}$ (0.23)			$55.53^{b,b}$ (0.80)
33	$5.21^{a,a}$ (1.67)	$28.51^{c,c}$ (1.58)	$47.53^{d,d}$ (0.27)	$29.44^{a,a}$ (2.64)			$56.26^{b,b}$ (0.50)

* Values show the mean and standard deviation of at least two replicates

[a–d] For the same blend and column data with the same first letter are statistically the same. A different letter indicates statistical difference (P # 0.10). Comparing data for the same blend and column of Tables 4 and 5, values with the same second letter are statistically the same. A different letter indicates statistical difference ($P < 0.10$)

Table 5 Parameters that describe the isothermal crystallization and corresponding melting profile of the selected blends with PH-SBO. Melting after isothermal crystallization at the indicated crystallization temperature (T_{Cr}). Legends as indicated in the text

T_{Cr} (°C)	t_i * (min)	ΔH_{Cr} (J/g)	T_{pk1} (°C)	ΔH_{pk1} (J/g)	T_{pk2} (°C)	ΔH_{pk2} (J/g)	T_M (°C)
Blend 5							
26	$1.32^{a,a}$ (0.03)	$18.06^{a,b}$ (1.17)	$40.57^{a,a}$ (0.41)	$9.58^{a,b}$ (0.50)	$49.59^{-,a}$ (0.00)	$1.43^{-,b}$ (0.20)	$56.20^{a,b}$ (0.34)
28	$3.15^{a,a}$ (0.18)	$22.03^{b,c}$ (2.61)	$43.85^{b,b}$ (0.11)	$19.69^{b,c}$ (2.03)			$52.38^{b,b}$ (0.96)
30	$4.30^{b,b}$ (0.21)	$18.88^{a,b}$ (1.42)	$44.31^{c,d}$ (0.01)	$16.55^{c,c}$ (0.40)			$53.64^{c,b}$ (0.96)
32	$8.06^{c,c}$ (3.53)	$15.01^{c,d}$ (0.49)	$46.59^{d,f}$ (0.57)	$16.26^{c,c}$ (0.33)			$55.00^{d,c}$ (0.06)
Blend 7							
23	$2.36^{a,a}$ (0.08)	$13.00^{a,b}$ (0.66)	$34.47^{a,a}$ (0.04)	$7.42^{a,a}$ (0.24)	$46.54^{a,a}$ (0.04)	$2.07^{a,b}$ (0.10)	$52.67^{a,a}$ (0.28)
24	$2.57^{a,a}$ (0.12)	$12.59^{a,b}$ (1.93)	$38.48^{b,c}$ (1.36)	$10.85^{b,c}$ (1.85)	$49.37^{b,c}$ (2.57)	$0.21^{b,c}$ (0.21)	$54.56^{b,c}$ (1.99)
26	$4.17^{b,b}$ (0.02)	$11.65^{a,c}$ (0.46)	$42.80^{c,c}$ (0.18)	$13.32^{c,c}$ (0.06)			$52.67^{a,a}$ (0.82)
28	$9.39^{c,d}$ (0.55)	$9.33^{b,c}$ (0.38)	$44.32^{d,d}$ (0.23)	$9.58^{d,c}$ (0.57)			$54.13^{b,b}$ (0.82)
Blend 10							
30	$3.70^{a,a}$ (0.11)	$24.00^{a,b}$ (0.12)	$45.51^{a,b}$ (0.08)	$22.47^{a,b}$ (1.17)			$55.80^{a,b}$ (0.99)
31	$3.36^{a,a}$ (0.34)	$24.24^{a,c}$ (0.22)	$45.97^{b,c}$ (0.20)	$21.96^{a,b}$ (1.20)			$56.00^{a,b}$ (0.87)
32	$4.75^{a,a}$ (2.74)	$21.82^{b,c}$ (0.54)	$46.29^{c,c}$ (0.14)	$23.92^{a,b}$ (0.14)			$54.65^{b,b}$ (0.35)
33	$11.49^{b,b}$ (0.37)	$19.71^{c,d}$ (0.88)	$47.99^{d,e}$ (0.21)	$26.13^{a,b}$ (0.01)			$57.35^{c,b}$ (0.70)

* Values show the mean and standard deviation of at least two replicates

[a–d] For the same blend and column data with the same first letter are statistically the same. A different letter indicates statistical difference (P # 0.10). Comparing data for the same blend and column of Tables 4 and 5, values with the same second letter are statistically the same. A different letter indicates statistical difference ($P < 0.10$)

previously suggested, blend 5 with or without TAG with *trans*-fatty acids might develop a different polymorph when crystallized at 26 °C than the one formed at T_{Cr} = 28 °C. We will return to this point later in the paper.

Blend 10 showed a particular behavior since the *trans*-free SBO blend showed higher yield stress than the PH-SBO blend (Fig. 4b). Blend 10 had the highest concentration of palm stearin and equivalent quantities of SBO

and coconut oil (Table 1). As suggested above, the incorporation of unsaturated *trans* TAG into the crystal structure developed by saturated TAG reduced the structural order of the crystals. Such phenomenon might affect the crystal network structure and, subsequently, the rheological properties. The incorporation of saturated medium chain TAG (i.e., LaLaLa from coconut oil) into the crystal structure, might further modify the organization of the crystal network and hence the rheology of the crystallized blend. As a result, blend 10 with *trans*-free SBO had higher yield stress than blend 10 with PH-SBO (Fig. 4b). The behavior of ΔH_{Cr} provided additional evidence of the *trans* TAG and medium chain TAG effect on crystal structure. This since blend 10 at all T_{Cr}'s observed the larger difference between ΔH_{Cr} values in PH-SBO systems and *trans*-free SBO systems (Tables 4 and 5). The blends with lower concentration of palm stearin (i.e., blends 5 and 7) also showed lower ΔH_{Cr} with PH-SBO (Table 5) than with *trans*-free SBO (Table 4). However, in these blends the overall effect of *trans* TAG and saturated medium chain TAG on the crystal structure might be not large enough to modify the crystal network organization and, subsequently, the σ^* profile.

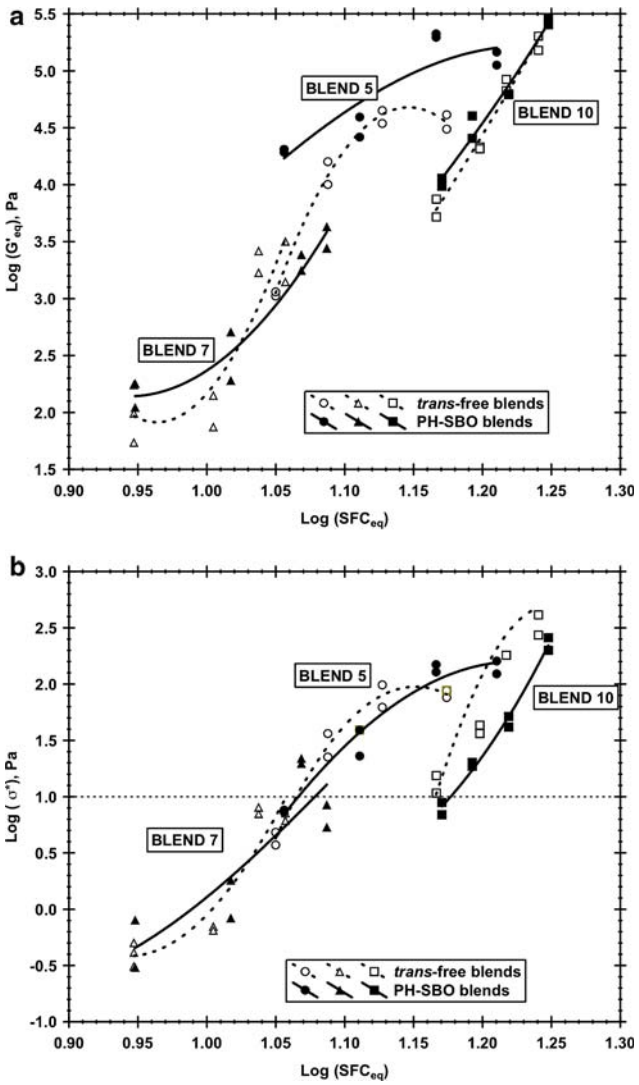

Fig. 4 G_{eq}' (**a**) and σ^* (**b**) profiles of the selected blends as a function of solid fat content at equilibrium (SFC_{eq}). The *dotted line* in the σ^* profile (**b**) shows the stress force (i.e., 10 Pa) used for the creep and recovery measurements

The microstructure of the blends was studied by PLM. However, since blend 7 provided the lower rheological properties and an apparent texture too soft to be considered useful for confectionary coatings, the PLM's discussion was restricted just to blends 5 and 10. PLM's for blends 5 and 10 showed a higher number of crystals with PH-SBO (Figs. 5b, d, f, h, 6b, d, f, h) than with *trans*-free SBO (Figs. 5a, c, e, g, 6a, c, e, g). This was more evident as T_{Cr} decreased. Additionally, for a particular blend, the lower the T_{Cr} the smaller the crystal size. Similar results were obtained with blend 7 (PLM results not shown). Rheological properties (i.e., G_{eq}' and σ^*) are directly associated with the volume fraction of solid fat through the mass fractal dimension of the crystal network, and have an inverse relationship with the diameter of the primary particles that form the network [23]. Additional variables affecting the rheology of a crystal network are the interaction forces associated with the van der Waals' forces between the structural elements of the network [24] and the crystal–crystal aggregation (i.e., sintering) [25]. Therefore, the differences in crystal size/number in the PLM results explained why blends with PH-SBO had higher G_{eq}' and σ^* than blends with *trans*-free SBO (Fig. 4). One exception was the σ^* profile of blend 10 (Fig. 4b) which was higher for the *trans*-free SBO system than the one with PH-SBO (Fig. 4b). This despite the fact the SFC_{eq} was the same with and without *trans* TAG at all T_{Cr}'*s*, and similar elastic profiles were provided for both systems (Fig. 4a). No particular explanation was found to describe the particular rheological behavior of blend 10.

In contrast to blend 10, the lower SFC_{eq} and crystal number (Fig. 5) present in blend 5 with *trans*-free SBO system resulted in lower elastic properties and, to a lesser extent, lower yield values than with the PH-SBO system (Fig. 4). This phenomenon was more evident at the lower T_{Cr}'*s*, i.e., higher SFC_{eq}. Additionally, as suggested by the ΔH_{Cr} results (Tables 4 and 5), *trans* TAG decreased the structural order of the crystals developed by blend 5. However, the effect of *trans* TAG on the crystal structure was not large enough to alter the crystal network organization and, subsequently, the σ^* profile. Nevertheless, as previously indicated, at certain T_{Cr}'*s* blend 5 with or without *trans* TAG provided systems with similar rheological properties than blend 10. This, regardless the differences in SFC_{eq}, crystal structure and crystal

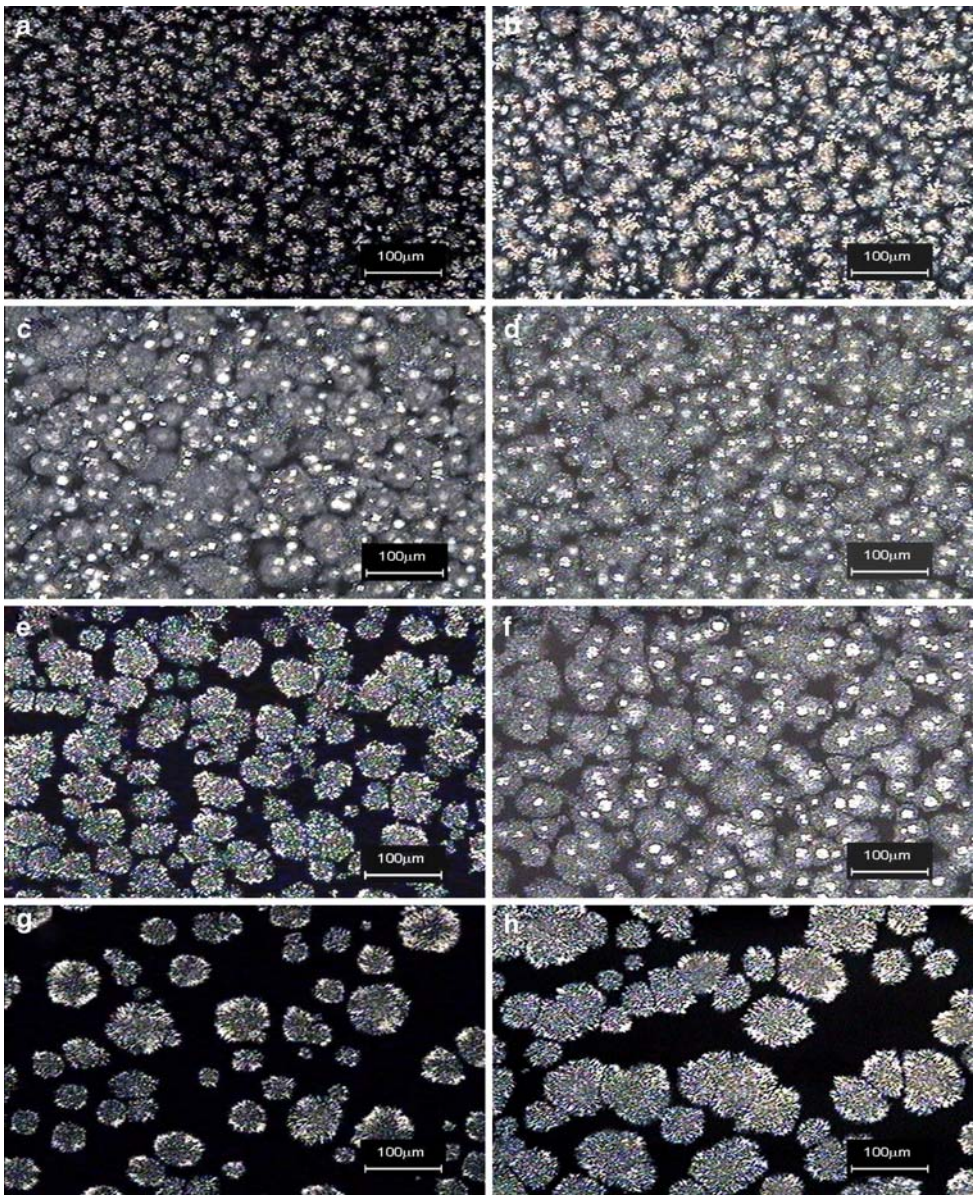

Fig. 5 Polarized light micrographs for blend 5 with *trans*-free SBO (**a, c, e, g**) or PH-SBO (**b, d, f, h**). The corresponding crystallization temperatures were 26 °C (**a** and **b**), 28 °C (**c** and **d**), 30 °C (**e**, **f**), and 32 °C (**g**, **h**)

network organization between blend 5 and 10. However, at high deformations the rheological behavior of blends 5 and 10 crystallized with or without *trans* TAG might be different.

Large Deformation Rheology

The creep profiles of the blends after 200 min of isothermal crystallization show the progressive deformation of the crystal network under constant stress (i.e., 1 min at 10 Pa). Upon release of the stress, the strain of the crystallized blend exhibited an instantaneous recovery followed by a progressive decrease of deformation until attaining a constant non-zero value, i.e., after deformation the blends never attained full recovery (Figs. 7, 8). The creep and recovery profiles of the blends investigated depended on T_{Cr}. The blends 5 and 10, with and without PH-SBO crystallized at the higher T_{Cr}'*s*, underwent full deformation with the evident rupture of the microstructure (data not show). Blend 7 showed the same rheological behavior at all T_{Cr}'*s* investigated (data not show). The PLM'*s* corresponding to blend 5 at a T_{Cr} of 32 °C are shown in Fig. 5g and 5h, and for blend 10 at a T_{Cr} of 33 °C in Fig. 6g and h. These results agreed with the σ^* profile shown in Fig. 4b, i.e., the force applied for the creep measurements [10 Pa; $\text{Log}(\sigma^*) = 1.0$] was higher than the yield stress for the blends at the corresponding T_{Cr}'*s* (see dotted line in Fig. 4b). In contrast, independent of the use of *trans*-free SBO or PH-SBO, blend 5 crystallized at 30 °C and blend 10 crystallized at 32 °C showed the higher deformation and the lower extent of recovery with respect to the same

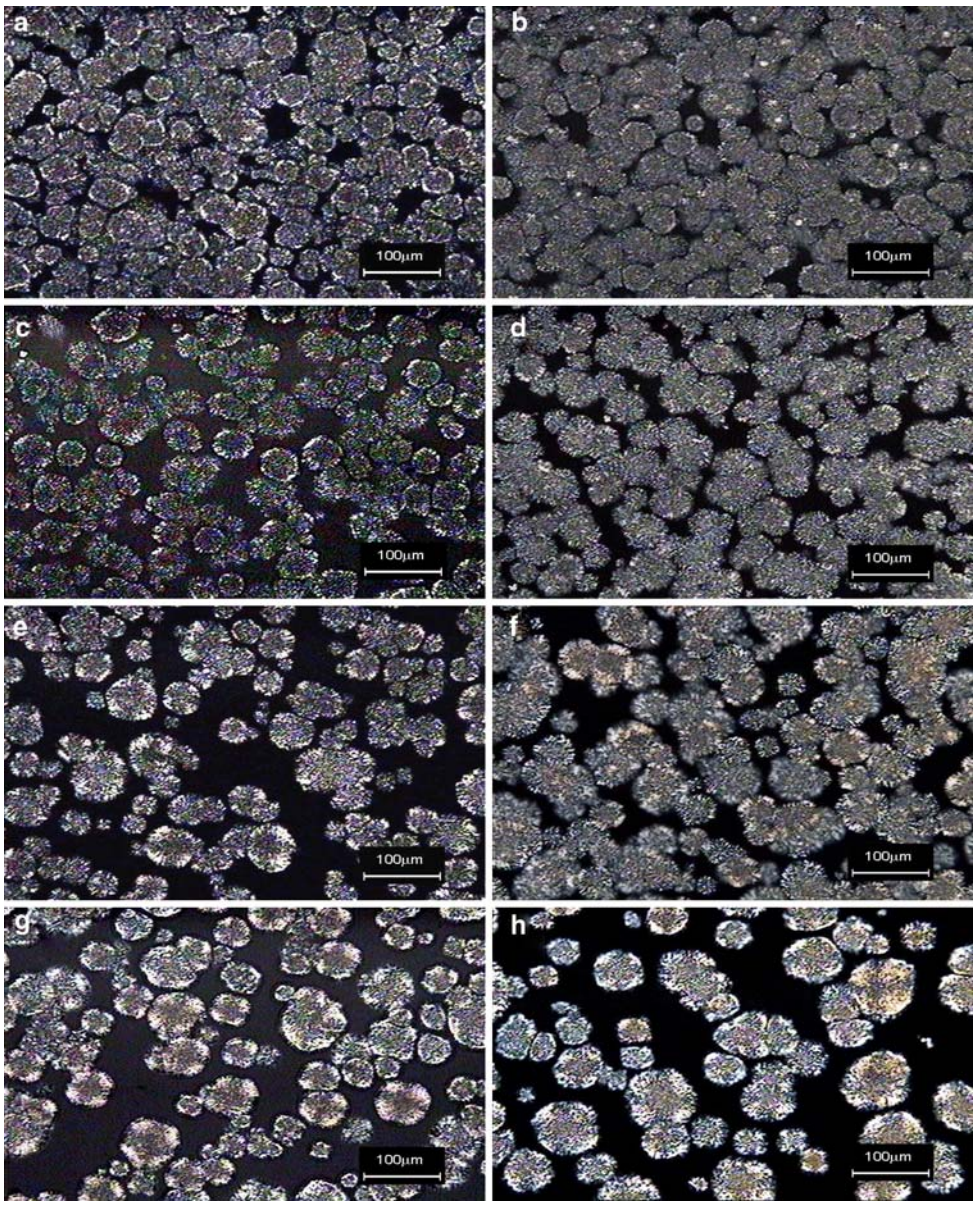

Fig. 6 Polarized light micrographs for blend 10 with *trans*-free SBO (**a, c, e, g**) or PH-SBO (**b, d, f, h**). The corresponding crystallization temperatures were 30 °C (**a** and **b**), 31 °C (**c** and **d**), 32 °C (**e**, **f**), and 33 °C (**g**, **h**)

blends crystallized at lower T_{Cr}'s. This phenomenon was more evident in blends with PH-SBO (Fig. 8) than with *trans*-free SBO (Fig. 7), particularly in the formulations containing coconut oil (i.e., blend 10, Fig. 8b). These results were explained considering the effect of *trans* TAG and saturated medium chain TAG on the crystal network organization and rheological properties.

The creep and recovery profile for crystallized systems is a direct measurement of the viscoelastic properties that in turn depend on the solid mass and microstructural organization of the systems. The PLM's for blends 5 and 10 with PH-SBO or *trans*-free SBO showed crystal networks formed by higher number of crystals of smaller size as T_{Cr} decreased (i.e., blend 10 with PH-SBO Fig. 6f, d, b; and blend 10 with *trans*-free SBO, Fig. 6e, c, a). The corresponding creep and recovery profiles for these blends showed lower deformation and higher extent of recovery as T_{Cr} decreased. In general, blend 10 prepared with *trans* TAG provided crystallized systems with softer textures that the corresponding *trans*-free blend, particularly at the higher T_{Cr} (i.e., 32 °C). This since in the *trans*-free blends the creep profile was significantly lower and recovery was higher (Fig. 7b) than in the blends with PH-SBO (Fig. 8b). These results agreed with the G_{eq}' and σ^* profiles (Fig. 4). Since the SFC_{eq} was the same in both types of blends ($P < 0.05$), the difference in their rheological properties had to be associated with structural differences in the crystal network. However, no particular structural differences were observed between the PLM for blend 10 with *trans*-free SBO (Fig. 6e, c, a) and the PLM with PH-SBO

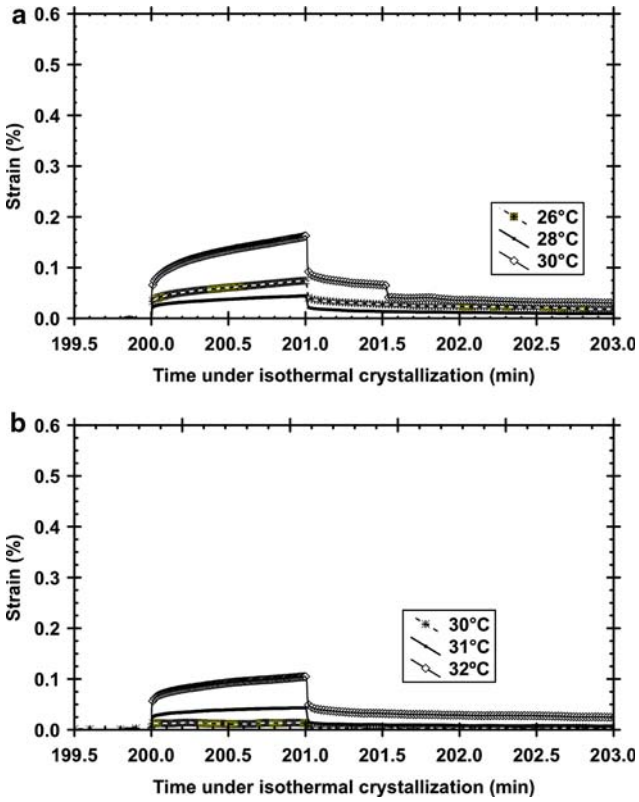

Fig. 7 Creep and recovery profiles at different crystallization temperatures for blend 5 (**a**) and blend 10 (**b**) with *trans*-free SBO

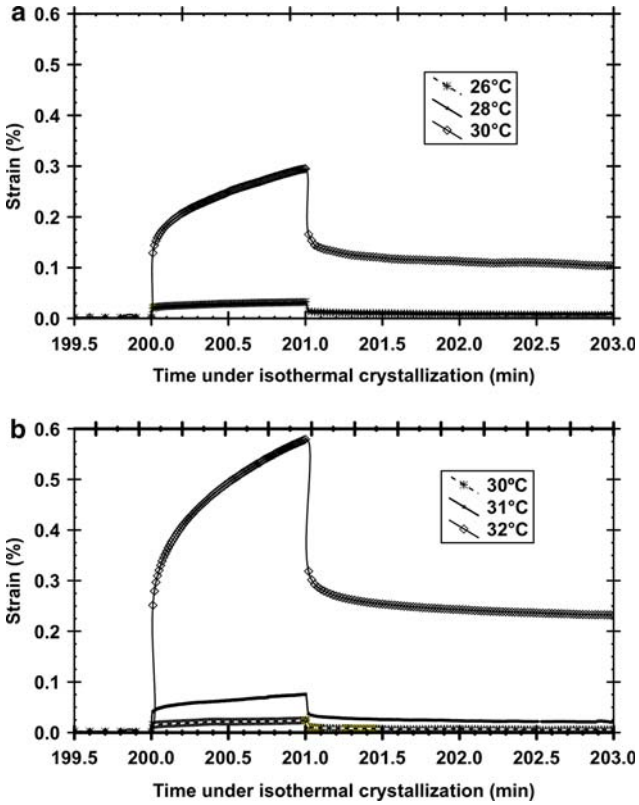

Fig. 8 Creep and recovery profiles at different crystallization temperatures for blend 5 (**a**) and blend 10 (**b**) with PH-SBO

(Fig. 6f, d, b). In contrast to blend 10, blend 5 with PH-SB crystallized at 30 °C showed higher deformation and lower extent of recuperation (Fig. 8a) than the corresponding *trans*-free blend (Fig. 7a). Additionally, at 28 °C blend 5 with *trans*-free SBO showed lower deformation than the one crystallized at 26 °C (Fig. 7a). This, regardless the higher SFC_{eq} present at T_{Cr} of 26 °C ($P < 0.05$). However, blend 5 with PH-SBO crystallized at the same T_{Cr}'s showed the same rheological profiles (Fig. 8a). The PLM'*s* suggested that the different rheological behavior observed by blend 5 with PH-SBO and with *trans*-free SBO, was associated with changes in crystal morphology and crystal network organization occurring in the blends at different T_{Cr}. Blend 5 with *trans*-free SBO showed a drastic change in crystal morphology and crystal network organization when T_{Cr} decreased from 30 °C (Fig. 5e) down to 28 °C (Fig. 5c) and from here down to 26 °C (Fig. 5a). In contrast, blend 5 with PH-SBO showed these changes when T_{Cr} decreased from 32 °C (Fig. 5h) to 30 °C (Fig. 5f) and then from 28 °C (Fig. 5d) down to 26 °C (Fig. 5b). Such changes in crystal morphology might be associated with polymorphic changes. However, no X-ray analyses were done to confirm this. Then, the polymorphism that probably occurred in blend 5 as a function of T_{Cr} and their associated effect on the crystal network structure can explain the difference in creep and recovery behavior between the systems with PH-SBO and the ones with *trans*-free SBO (Figs. 7a, 8a). As reported in other investigations [26, 27], rheological properties of crystallized TAG systems depend on SFC, crystal size and its polymorphic state, this as affected by the physicochemical characteristics of TAG in the liquid phase.

Finally, we have to remember that the blends investigated were selected based on their high melting temperatures. This, since their aim of use is in the development of high melting temperature confectionary coatings. Blends 5 and 10 with and without *trans* TAG showed $T_M = s$ between 52.4 and 57.4 °C and T_{pk1}'s between 40.4 and 48.0 °C (Tables 4 and 5). In particular, under low deformations blends 5 and 10 with PH-SBO at the T_{Cr}'*s* of 30 and 32 °C, respectively, provided similar G_{eq}' [blend 5, 32.72×10^3 Pa (s.d. = 9.22×10^3 Pa); blend 10, 32.86×10^3 Pa (s.d. = 10.34×10^3 Pa); $P < 0.05$]. However, the same blends had different yield stress values ($P < 0.05$), with $\sigma^* = 31.04$ Pa (s.d. = 11.36 Pa) for blend 5 and $\sigma^* = 19.41$ Pa (s.d. = 1.15 Pa) for blend 10. In consequence, the creep and recovery profiles for blend 10 at 32 °C showed higher deformation with lower recovery than blend 5 at 30 °C (Fig. 8). Then, regardless the higher SFC_{eq} of blend 10 with PH-SBO [15.68% (s.d. = 0.14%)] in comparison with

blend 5 with PH-SBO [12.91% (s.d. = 0.06%)], blend 10 provided a softer texture than blend 5. All blends with *trans*-free SBO crystallized at any of the T_{Cr}'*s* investigated, provided systems with rheological properties that would result in harder textures that the ones provided by blends 5 and 10 with PH-SBO crystallized at 30 and 32 °C, respectively. These results pointed out the main functional shortcomings when replacing *trans* fats with *trans*-free formulations, i.e., limited plasticity and harder texture. Nevertheless, blend 5 with *trans*-free SBO at T_{Cr}'s of 26 and 30 °C and blend 10 with *trans*-free SBO at the T_{Cr} of 32 °C, provided rheological properties that ought to result in softer textures than the corresponding systems with PH-SBO. Thus, blend 5 with *trans*-free SBO at T_{Cr}'s of 26 and 30 °C had G_{eq}' of 35.99×10^3 Pa (s.d. = 7.26×10^3 Pa) and 12.99×10^3 Pa (s.d. = 4.15×10^3 Pa), respectively. In contrast, blend 10 with *trans*-free SBO at T_{Cr} of 32°C had a G_{eq}' of 21.06×10^3 Pa (s.d. = 0.61×10^3 Pa). The corresponding σ^* values were 81.85 Pa (s.d. = 8.25 Pa), 29.45 Pa (s.d. = 9.81 Pa), and 39.82 Pa (s.d. = 4.91 Pa), respectively. The corresponding creep and recovery profiles for these *trans* free blends showed higher deformation and lower extent of recuperation than the corresponding blends with PH-SBO (Figs. 7, 8). Therefore, *trans*-free formulations of blend 5 crystallized at 26 and 30 °C and blend 10 crystallized at 32 °C might provide crystallized systems with softer textures than the ones obtained with the corresponding PH-SBO blends. In conclusion, knowledge of the rheological properties under low and high stress forces provide vital information when comparing the functionality of crystallized TAG systems (i.e., confectionary coatings) with and without TAG with *trans* fatty acids.

Acknowledgments The investigation was supported by grant # 48273-Z from CONACYT. The technical support from Concepcion Maza-Moheno and Elizabeth Garcia-Leos is greatly appreciated.

References

1. Jang ES, Jung MY, Mind DB (2005) Hydrogenation for low *trans* and high conjugated fatty acids. J Food Sci 1:22–30
2. Mensink RP (2005) Metabolic and health effects of isomeric fatty acids. Curr Opin Lipidol 16:27–30
3. Stender S, Dyerberg J (2004) Influence of *trans* fatty acids on health. Ann Nutr Metab 48:61–66
4. Ascherio A, Stampfer MJ, Willett WC (1999) Trans fatty acids and coronary heart disease, http://www.hsph.harvard.edu/reviews/transfats.pdf
5. Manku MS, Horrobin DF, Morse N, Kyte V, Jenkins K, Wright S, Burton JL (1982) Reduced level of prostaglandin precursors in the blood of atopic patients: defective Δ-6-desaturase function as a biochemical base for atopy. Prostaglandins Leukot Med 9:615–628
6. Kodali RD, List GR (Eds) (2005) *Trans* fats alternatives. AOCS, Champaign
7. Petraskaite V, de Greyt WF, Kellens MJ, Huyghebaert AD (1998) Physical and Chemical properties of *trans*-free products by chemical Interesterification of vegetable oil blends. J Am Oil Chem Soc 75:489–493
8. Petraskaite V, de Greyt WF, Kellens MJ, Huyghebaert AD (1998) Chemical interesterification of vegetable oil blends: optimization of process parameters. Oleagineuz Corp Gras Lipides 5:65–69
9. Reddy SY, Jeyarani T (2001) *Trans*-free bakery shortenings from Mango Jernel and Mahua fats by fractionation and blending. J Am Oil Chem Soc 78:635–640
10. Berger KG, Idris NA (2005) Formulation of zero-*trans* acid shortenings and margarine and other food fats with products of the oil palm. J Am Oil Chem Soc 82:775–782
11. Macher M, Holmquivst A (2001) Hydrogenation of palm oil in a near-critical and supercritical propane. Euro J Lipid Sci Technol 101:81–84
12. Mondal K, Lalvani SB (2003) Electrochemical hydrogenation of canola oil using hydrogen transfer agent. J Am Oil Chem Soc 80:1135–1141
13. Yang ES, Jung MY, Min DB (2005) Hydrogenation for low trans and high conjugated fatty acids. J Food Sci 1:22–30
14. Seize K (2005) Sourcing ideal *trans*-free Oils. Funct Foods Nutraceuticals, July:36–38
15. Ascherio A, Katan M, Zock PL, Stampfer MJ, Willett WC (1999) *Trans* fatty acids and coronary heart diseases. N Engl J Med 340:1994–1998
16. Pérez-Martínez D, Alvarez-Salas C, Morales-Rueda J, Toro-Vazquez JF, Charó-Alonso M, Dibildox-Alvarado E (2005) The effect of supercooling on crystallization of cocoa butter-vegetable oil blends. J Am Oil Chem Soc 82:627–632
17. Ruguo H (1999) Food product design, Chap 4. Food recipe modeling and optimization. Technomic Publishing Company Inc., Pennsylvania, pp 125–175
18. Toro-Vazquez JF, Dibildox-Alvarado E, Charó-Alonso MA, Herrera-Coronado V, Gómez-Aldapa CA (2002) The Avrami index and the fractal dimension in vegetable oil crystallization. J Am Oil Chem Soc 79:855–866
19. AOCS Method (1998) Ce 1f-96, in Official Methods and Recommend Practices of the American Oil Chemist's Society, 5th edn. AOCS, Champaign
20. Sonoda T, Takata Y, Ueno S, Sato K (2004) DSC and synchrotron-radiation X-ray diffraction studies on crystallization and polymorphic behavior of palm stearin in bulk and oil-in-water emulsion states. J Am Oil Chem Soc 81:365–373
21. Hagemann JW, Tallent WH (1972) Differential scanning calorimetry of single acid triglycerides: effect of chain length and unsaturation. Ibid 49:118–123
22. Kodali DR, Atkinson D, Small DM (1987) Structure and polymorphism of 18-carbon fatty acid triacylglycerols: effect of unsaturation and substitution in the 2-position. J Lipid Res 28:403–413
23. Narine SS, Marangoni AG (1999) Mechanical and structural model of fractal networks of fat crystals at low deformations. Phys Rev E 60:6991–7000
24. Marangoni AG (2000) Elasticity of high-volume-fraction fractal aggregate networks: a thermodynamic approach. Phys Rev B 62:13951–13955
25. Johansson D, Bergenståhl B (1992) The influence of food emulsifiers and fat and sugar dispersions in oils. II. Rheological, colloidal forces. J Am Oil Chem Soc 69:718–727
26. Pérez-Martínez D, Alvarez-Salas C, Charó-Alonso MA, Dibildox-Alvarado E, Toro-Vazquez JF (2007) The cooling rate effect on the microstructure and rheological properties of *blends* of cocoa butter with vegetable oils. Food Res Int 40:47–62
27. Shi Y, Liang B, Hartel RW (2005) Crystal morphology, microstructure and textural properties of model lipid systems. J Am Oil Chem Soc 82:399–408